Lightweight Co_3O_4/CC Composites with High Microwave Absorption at Low Frequency

Bing An , Mei Wu , Xinhuang Yang , Zengming Man , Xiaohui Liang * , Chunyang Feng *

Posted Date: 1 June 2023

doi: 10.20944/preprints202306.0095.v1

Keywords: Low frequency; Co3O4/CC; Co-MOFs/CC; thinner thickness

Article

Lightweight Co_3O_4/CC Composites with High Microwave Absorption at Low Frequency

Bing An [1,2], Mei Wu [1], Xinhuang Yang [1], Zengming Man [3], Xiaohui Liang [1,*] and Chunyang Feng [1,*]

[1] Hangzhou Dianzi University, Hangzhou, 310018, PR China
[2] Xiamen University, Xiamen, Fujian 361005, PR China
[3] National Engineering Lab for Textile Fiber Materials & Processing Technology, Zhejiang Sci-Tech University, Hangzhou 310018, P. R. China
* Correspondence: xhliang@hdu.edu.cn (X.L.); sam@hdu.edu.cn (C.F.)

Abstract: With the rapid development of electronic and communication technology in military radar, the demand for microwave absorbing materials in low-frequency with thin layer is growing increasingly. In this study, flexible Co_3O_4/CC (carbon cloth) composites derives from Co-MOFs (metal-organic frameworks)/CC are prepared by hydrothermal and thermal treatment processes. The flexible precursors of Co-MOFs/CC are calcined with different calcination temperatures, which the material structure, dielectric properties and microwave absorption performance are changed. With the increase of calcination temperature, the minimum reflection loss of the corresponding Co_3O_4/CC composites gradually moves to the lower frequency with thinner thickness. In addition, the Co_3O_4/CC composites with 25 wt% filler loading ratio exhibit the minimum reflection loss (RL) of -46.59 dB at 6.24 GHz with 4.2 mm thickness. When the thickness is 3.70 mm, the effective absorption bandwidth is 3.04 GHz from 5.84 to 8.88 GHz. This study not only proves that the composite Co_3O_4/CC is a kind of outstanding microwave absorbing material with better flexibility, but also provides a useful inspiration for the low frequency and broadband microwave absorbing material.

Keywords: Low frequency; Co_3O_4/CC; Co-MOFs/CC; thinner thickness

1. Introduction

With the rapid development of science and technology, the influences of electromagnetic radiation on human body and environment have attracted extensive attention. In terms of this background, the development of microwave absorption materials can resist electromagnetic radiation and it has become a research hotspot in the world [1]. An ideal microwave absorbing material should have excellent properties such as light weight, thin thickness, strong reflection and broad effective absorption bandwidth [2]. In recent years, researchers have studied a variety of ideal microwave absorbing materials including the magnetic loss materials and dielectric loss materials. For instance, Wang et al. synthesized the Fe_3O_4@SnO_2/RGO ternary composites with an efficient and rapid three-step method improving the impedance matching and obtaining excellent electromagnetic wave absorption performance [3]. Moreover, ZnO [4], Fe2O3/N-Graphene/CNTs [5], composite nonlinear feedback (CNF)/SiO_2 [6] and MOFs derivatives [7] et al. have also been widely developed to improve the attenuation characteristics of electromagnetic waves. In view of the loss mechanism of electromagnetic waves, it is generally easier to achieve strong broadband microwave absorption at high frequencies. However, the absorbing materials at low-frequency normally have thick thickness and narrow frequency bandwidth, which is difficult to meet the needs of practical application. Therefore, it is essential to research lightweight thinner layer with wide bandwidth absorber at low frequency.

Among a large number of lightweight electromagnetic absorption materials, MOFs derivatives have been extensively manufactured because of their variety of metals, diversity of morphology and highly surface areas [8-11]. For example, Ma et al. synthesized TiO_2/C nano-porous carbon composites by pyrolysis of MIL-125 (Ti-based MOFs), which exhibited maximum reflection loss of -49.60 dB with

 doi:10.20944/preprints202306.0095.v1

thinner thickness of 1.6 mm and obtained 4.6 GHz effective absorption bandwidth [12]. In addition, Shi et al. studied the nanoporous Co_3O_4 nanosheets derived from Co-MOFs, when the matching thickness is 2.5 mm, the maximum reflection loss can reach -32 dB, and the effective absorption band width can reach 4.2 GHz because of its better impedance matching of the composites [13]. Besides, Liu et al. also designed Co-MOFs derivatives to improve the absorption performance in the low frequency. The better impedance matching has been achieved with the Co/C composite, which minimum reflection loss value was about -20 dB and the effective absorption bandwidth reached 3.84 GHz in C-band frequency range [14]. Therefore, MOFs derivatives could obtain broadband absorption performances with thinner thickness in low frequency. In addition, MOFs can be combined with other functional materials to improve the microwave absorption performance. For example, Yang et al. fabricated SiC/Ni/NiO/C by annealing SiC/Ni-MOFs nanoparticles, which minimal RL value reached -50.52 dB [15]. Furthermore, Fe/Fe_3C/C derived from MIL-101-Fe and MIL-88-Fe was obtained by Miao et al. The minimum RL of the composites is -59.2 dB with a thickness of 4.32 mm and the effective bandwidth achieve 6.5 GHz with 2 mm [16]. Thus, the combination of MOFs derivatives and another material is better for the loss of microwave.

In recent decades, carbon cloth (CC) has been applied to various fields owing to its light weight, high strength, corrosion resistance and aging resistance [17-23]. Luo et al. prepared $NiSe_2$/CC as an electrode material without adhesive, which show good hydrogen evolution reaction performance and chemical stability in 0.5 mol/LH_2SO_4 solution [24]. Zhan et al. grow porous arrays of CoP nanoparticles derived from MOFs on carbon cloth using for effective alkaline hydrogen evolution [25]. Along with these, carbon cloth can also be used to prepare flexible microwave absorber. Che et al. made ZnO grow on CC flexible substrate, which constructed three-dimensional conductive network with multiple interfaces [26]. Moreover, Liu et al. grow of Co-MOF on conductive CC, which derived CC@NPC/CoS_2 composites of RL reaching -59.6 dB with 2.8 mm [27]. Based on the above, the carbon cloth can be combined with metal-organic framework materials for preparing excellent electromagnetic wave absorber with thin layer.

In this study, the Co_3O_4/CC derived from Co-MOFs/CC is synthesized, the result indicates that the absorbing properties of Co_3O_4/CC composite can be adjusted by controlling different calcination temperatures. When the calcination temperature is 500 °C, the Co_3O_4/CC composites showed an RL_{min} (minimum reflection loss) of -46.59 dB at 6.24 GHz with a filler loading ratio of 25 wt%. Furthermore, the Co_3O_4/CC material exhibits an effective microwave absorption bandwidth of 3.04 GHz from 5.84 GHz to 8.88 GHz with a thickness of 3.70 mm. Thus, the Co_3O_4/CC composite derived from the metal-organic framework/CC can be as a promising wide-band absorbing material with thin layer in low frequency.

2. Materials and Methods

2.1. Preparation of Precursors of Co-MOFs/CC

A piece of 2*2 cm^2 CC was placed in acetone cleaning by deionized water and ethanol, which was ultrasonicated for 20 min respectively and then dried in a vacuum oven at 60 °C for 6 h. The preparation of Co-MOFs/CC is as Figure 1, dissolving 432 mg cobalt nitrate hexahydrate, 300 mg terephthalic acid and 3 g PVP K30 (Polyvinylpyrrolidone K30) in a 60 mL mixture solution (deionized water: DMF: ethanol =1:1:1 v/v/v) and stirring vigorously with a blender until completely dissolved. Then put the cleaning CC into the bottom of the 100 mL Teflon autoclave, and transfer the mixture solution into it. Finally, the Teflon autoclave was heated in an oven at 150 °C for 10 hours, and the Co-MOFs/CC was obtained. The precursor of Co-MOFs/CC was obtained after washing with deionized water and ethanol for three times and drying in an oven at 60 °C for 12 hours.

2.2. Synthesis of Co_3O_4/CC Composites

The Co-MOFs/CC composite was heated to 300 °C, 400 °C, 500 °C respectively in a muffle furnace with a heating rate of 2 °C/min and heat two hours to obtain multilayer Co_3O_4/CC composites, named as S1, S2 and S3, respectively.

Preprints (www.preprints.org) | NOT PEER-REVIEWED | Posted: 1 June 2023 doi:10.20944/preprints202306.0095.v1

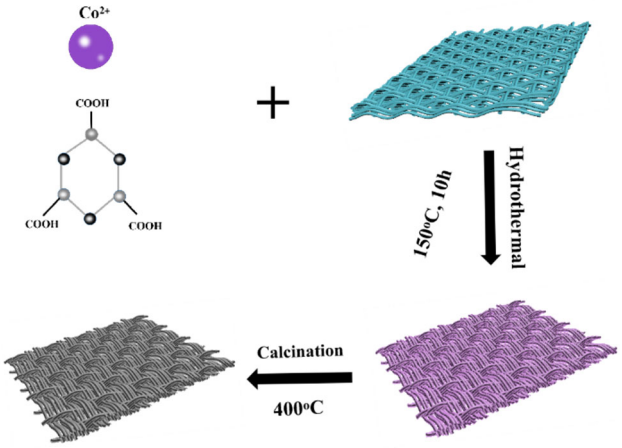

Figure 1. The structure diagram of experimental process.

2.3. Characterization and Measurement

The morphology of Co_3O_4/CC and pure CC was characterized by field emission scanning electron microscopy (FE-SEM, S-4800, Hitachi), X-ray diffractometer (XRD) was used to collect powder diffraction data in the range of 10-70 °C with Cu Kα radiation (λ=1.5418 Å). XPS was obtained by model PHI 5000 Versa Probe. Then, the relative complex permittivity and permeability in the frequency range of 2-18 GHz were measured by the Agilent PNA N5224A vector network analyzer with coaxial method and filler loading ratio of 25 wt%.

3. Results and Discussion

The sample phase composition and crystallinity of Co_3O_4/CC composites can be observed by XRD diffraction analysis. In order to detect the successful synthesis of Co_3O_4/CC, the XRD patterns of the composites are analyzed in Figure 2. The diffraction peaks of Co_3O_4 were observed at 31.27°, 36.85° and 44.81° for S1-S3, which are corresponding to (220), (311) and (400) lattice plane. In addition, obvious diffraction peaks of C were observed at 22.76° (120), 26.57° (103) and 29.31° (113), which proved the existence of Co_3O_4 and carbon [28]. At the same time, no other impurity peaks are observed, indicating that the sample has a high purity and crystallinity [29]. It is obvious that Co_3O_4/CC has been successfully synthesized.

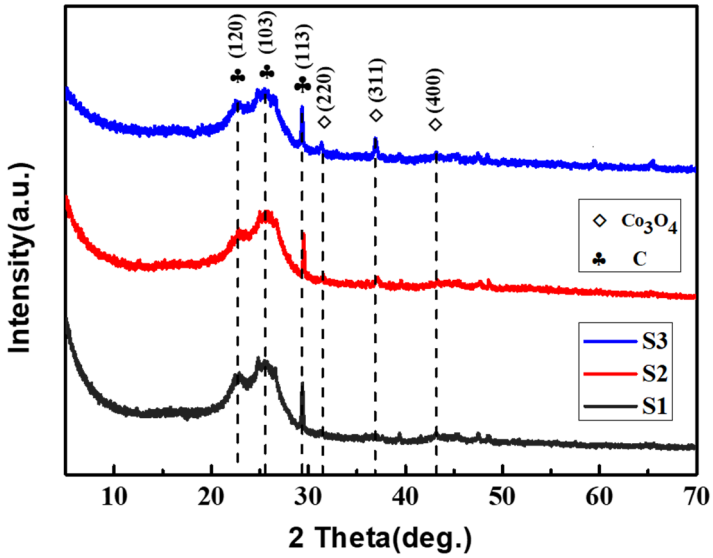

Figure 2. The XRD patterns of S1-S3.

 doi:10.20944/preprints202306.0095.v1

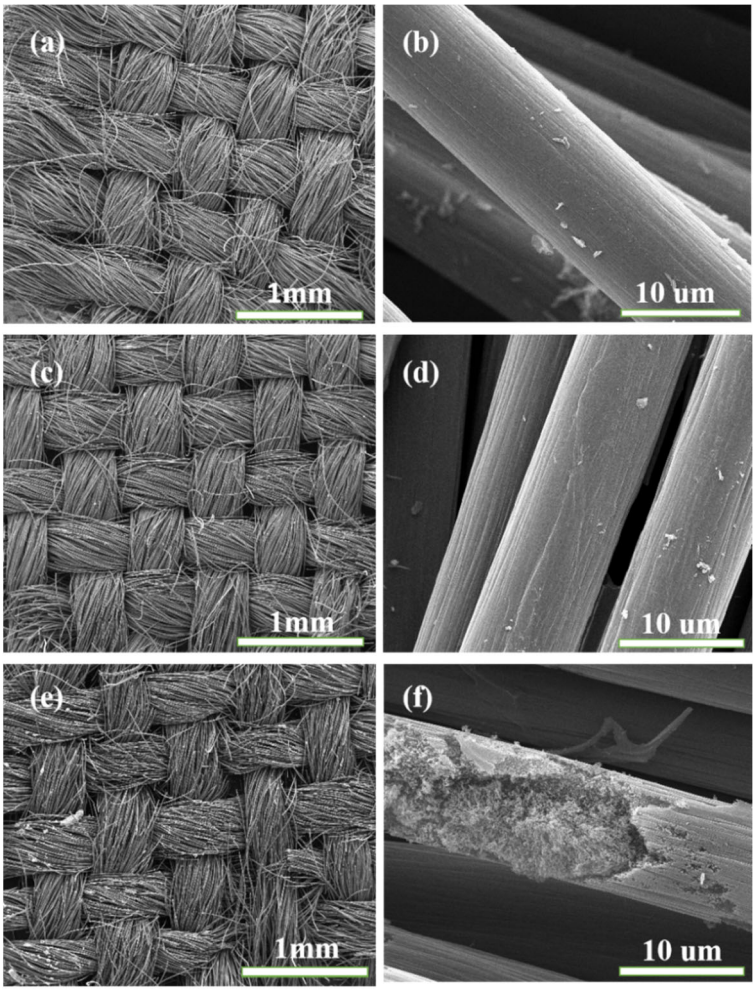

Figure 3. SEM images of (a-b) S1, (c-d) S2 and (e-f) S3.

The morphology of Co_3O_4/CC composites with different temperatures were characterized by SEM pictures, which were shown in Figure 3. It can be seen from Figure 3 that the morphology of the samples with three different temperatures is very similar, the cross arrangement of the cylindrical morphology is well maintained and the structure size is quite uniform. However, with the temperature increasing, the morphology of Co_3O_4/CC become roughly. In particularly, it can be seen from Figure 3f that most of the cylinder has been broken and presents a loose and porous structure, which may be caused by the collapse of the Co-MOFs. In addition, the surface of CC is relatively smooth and the floccule appears in the broken CC, which demonstrates the Co_3O_4 is grown inside of the CC. The floccule could provide loose and porous structure, which can offer more contact sites and increase the attenuation of electromagnetic waves.

Preprints (www.preprints.org) | NOT PEER-REVIEWED | Posted: 1 June 2023 doi:10.20944/preprints202306.0095.v1

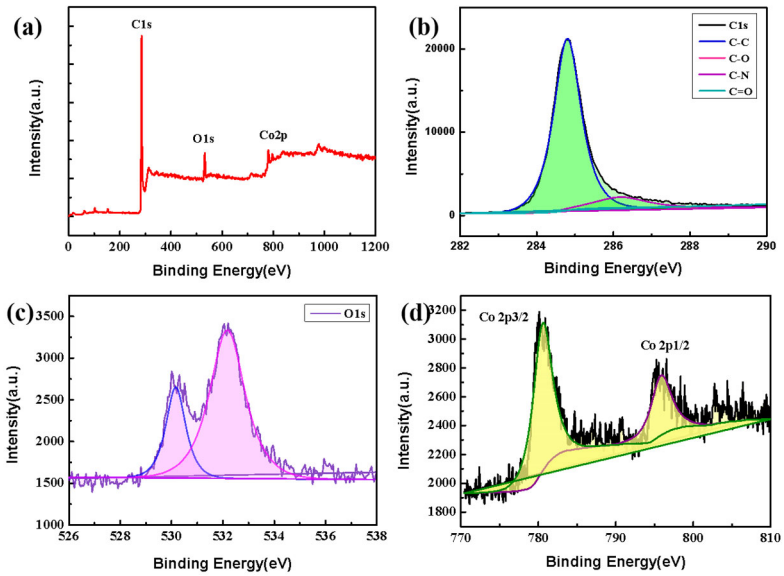

Figure 4. (a) XPS survey spectrum of S3; (b) C 1s, (c) O 1s and (d) Co 2p of core level spectrum in S3.

The valence states of elements in the composites can be clearly indicated by XPS [30]. The XPS results of Co_3O_4/CC are shown in Figure 4. Figure 4a shows the wide spectrum of Co_3O_4/CC composite material, and the Figure 4b-d shows the spectrum of C 1s, O 1s and Co 2p of S3 composite respectively. As can be seen from Figure 4b, two characteristic peaks appear in the C-1s spectrum of Co_3O_4/CC, which was peak-divided with the C-C/C=C peak appearing at 284.6 eV and the C-O peak emerging at 286.7 eV. It is obvious that the C-C/C=C bond signal is the strongest, which indicates that most of the precursor has become amorphous carbon after calcination and carbonization [31]. The results of XPS analysis in Figure 4c show that two characteristic peaks also appear in the O 1s spectrum of Co_3O_4/CC, in which the peaks are loading at 531.6 eV and 532.5 eV. In Figure 4d, the spectral peaks of Co 2P at 781.0 eV and 797.1 eV belong to Co 2P 3/2 and Co 2P 1/2, respectively [32]. The characteristic peaks can be attributed to cobalt nitrate hexahydrate and also indicates the presence of C and O elements.

Different calcination temperatures of precursor Co/CC could change the internal structure of Co_3O_4/CC composites, which affect the dielectric constant and magnetic permeability of the composite and adjust its microwave absorption property. In this study, we only pay attention to the dielectric characteristic analysis on account of the weak magnetism of the generated Co_3O_4/CC complex. The real parts (ε') and imaginary parts (ε'') of the complex dielectric constant are on behalf of the dielectric storage and dielectric loss capacity of the material, respectively [33]. It can be revealed from Figure 5 that the ε' of the Co_3O_4/ CC complex generally decreases with the increase of frequency. It's worth noting that the ε' increases several times after the high frequency part of 9 GHz, which is mainly bring from exchange resonance [34]. According to Debye theory, the real and imaginary parts of the complex dielectric constant can be expressed in the following form [35]:

$$\varepsilon' = \varepsilon_\infty + (\varepsilon_s - \varepsilon_\infty)/(1+\omega^2\tau^2) \quad (1)$$

$$\varepsilon'' = (\varepsilon_s - \varepsilon_\infty)\omega\tau/(1+\omega^2\tau^2) + \sigma_{ac}/\omega\varepsilon_0 \quad (2)$$

where ε_s represent the static permittivity, ε_∞ is the infinite static permittivity, ω belongs the angular frequency, τ is the polarization relaxation time, δ_{ac} is on behalf of the electrical conductivity and ε_0 represents the vacuum permittivity. According to equation (1), the decrease of the real part of the dielectric is independent of the increase of the angular frequency ω. The essence of this phenomenon is made from the existence of polarization relaxation at low frequency. Generally, it is important to note that the general relationship between the real part and imaginary part of the dielectric constant of the Co_3O_4/CC composite with three temperatures is S1 > S2 > S3. The reason why the complex

Preprints (www.preprints.org) | NOT PEER-REVIEWED | Posted: 1 June 2023 doi:10.20944/preprints202306.0095.v1

dielectric constant decreases gradually is that with the increase of calcination temperature, more and more Co_3O_4 is generated, which make the electrical conductivity gradually weakened of the Co_3O_4/CC.

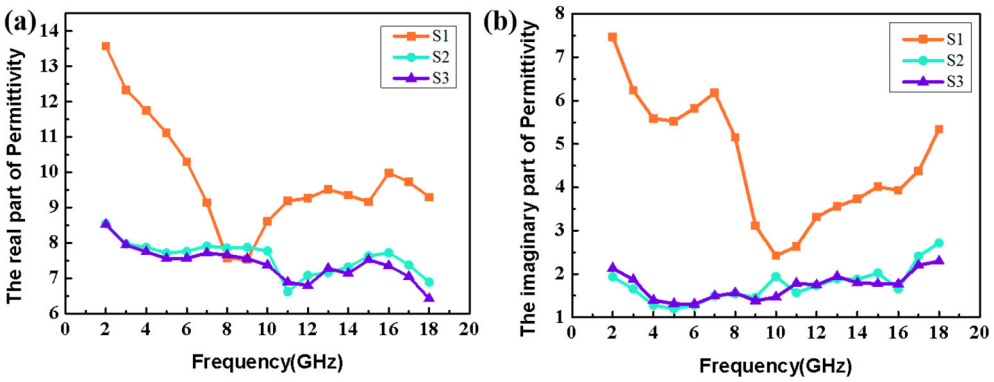

Figure 5. The real (a) and imaginary (b) parts permittivity of the Co_3O_4/CC complex with three temperatures.

After analyzing the complex permittivity of Co_3O_4/CC composite, the reflection loss of the generated composite is analyzed. Figure 6 shows the three-dimensional image of RL with different calcination temperatures and matching thickness, which can directly observe the RL value of Co_3O_4/CC composite. The calculation formulas for RL of electromagnetic wave are as follows:

$$Z_{in} = Z_0(\mu_r/\varepsilon_r)^{1/2} \tan \mathrm{h}\left[j(2\pi f d/c)\,(\varepsilon_r\mu_r)^{1/2}\right] \quad (3)$$

$$R_L = 20 \log\left(Z_{in} - Z_0\right)/\left(Z_{in} + Z_0\right) \quad (4)$$

where, Z_0 represents the impedance value of the free space. Figure 6a shows the three-dimensional (3D) RL of S1, and it can be seen that the minimum RL is -44.68 dB at 11.72 GHz with the thickness of 2.10 mm. Although the matching thickness of S1 is relatively thin, the frequency corresponding to the minimum reflection loss is still at the high frequency range (Ku band). The minimum reflection loss of S2 in Figure 6b is -33.95 dB, and the corresponding frequency and thickness are 5.4 GHz and 4.90 mm. The RL value of S3 is shown in Figure 6c, and the minimum RL can reach -46.59 dB at 6.24 GHz with a 4.2 mm thickness. It can be concluded that the frequency of the minimum RL gradually moves to low frequency with the increase of calcination temperature. According to Figure 6a, RL value is less than -10 dB in the frequency range of 10.76 to 14.16 GHz for S1, thus, the effective absorption band width of S1 is 3.4 GHz. Similarly, S2 (Figure 6b) has an effective absorption band width of 1.88 GHz in the frequency range of 4.52 ~ 6.4 GHz, while S3 (Figure 6d) has an effective absorption band width of 2.6 GHz with a frequency range of 5.12 ~ 7.72 GHz. It is well known that a good electromagnetic wave absorber should have large attenuation ability, superior impedance matching performance, minimum value of RL and a wide effective absorption band width and so on [36-37]. According to the above analysis, it's obvious that in low frequency area (< 6 GHz) the S3 have better reflection loss and thinner matching thickness. Therefore, the Co_3O_4/CC complexes with calcination temperature of 500 °C is suitable for the microwave absorbing materials in low frequency.

Preprints (www.preprints.org) | NOT PEER-REVIEWED | Posted: 1 June 2023 doi:10.20944/preprints202306.0095.v1

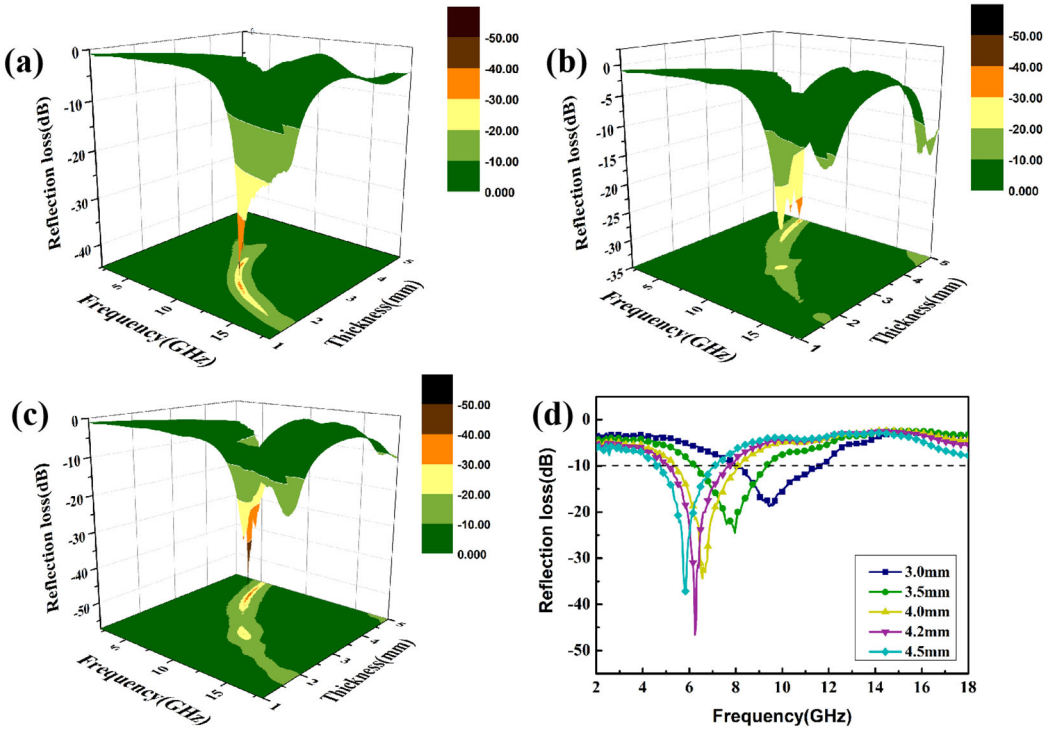

Figure 6. 3D plots of RL values for Co_3O_4/CC with different calcination temperatures of (a) S1, (b) S2, (c) S3 in the frequency range of 2-18 GHz; (d) the RL values of S3 with different thicknesses.

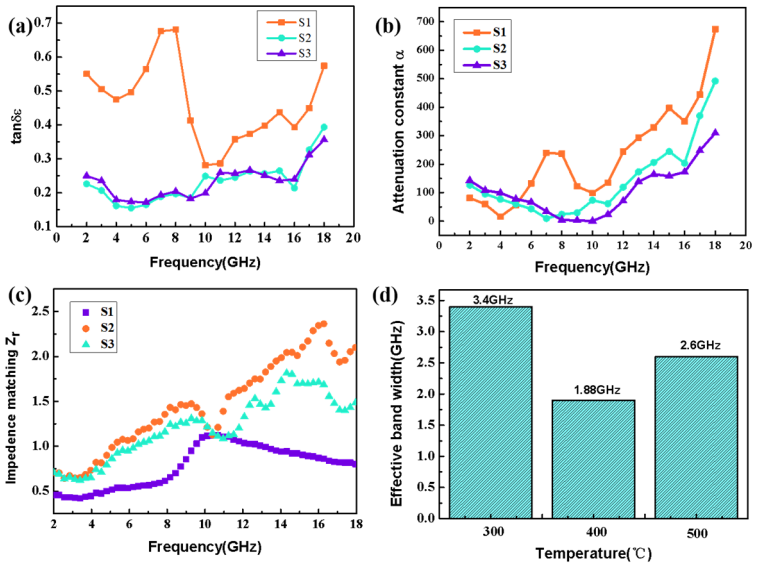

Figure 7. Frequency dependence of (a) tan δ_ε, (b) α and (c) Z_r of S1-S3; (d) effective absorption bandwidth with three calcination temperatures.

In order to further explore the mechanism why the Co_3O_4/CC composites have different absorbing properties with different calcination temperatures, the dielectric loss, attenuation ability of electromagnetic wave and impedance matching of the composites were further analyzed in this study. The dielectric loss is usually presented by the loss tangent of permittivity, the higher loss tangent indicating better dielectric loss. The loss tangent of permittivity can be expressed in the following formula [38]:

$$tan\,\delta_\varepsilon = \varepsilon'' / \varepsilon' \quad (5)$$

Preprints (www.preprints.org) | NOT PEER-REVIEWED | Posted: 1 June 2023 doi:10.20944/preprints202306.0095.v1

Figure 7a presents the variation of dielectric loss of Co_3O_4/CC composites with different calcination temperatures. In general, tan δ_ε with three temperatures demonstrate an upward trend in terms of the increase of frequency. Besides, a few relaxation peaks appear in low frequency, which proves that there are polarization relaxations in low frequency indicating better microwave absorption. For S1-S3 samples, the S1 composite has higher dielectric loss.

In addition to the dielectric loss, the attenuation factor α [39] and impedance matching Z_r [40] also play vital roles in the performance of electromagnetic wave absorption. Attenuation α refers to the amplitude or power attenuation in the electromagnetic wave transmission process, which is related to the dielectric loss. As can be seen from Figure 7b, the magnitude relationship of the attenuation ability of the three samples is $\alpha_{S1}>\alpha_{S2}>\alpha_{S3}$, indicating the S1 sample has better attenuation ability for electromagnetic waves. This is because with the enhance of calcination temperature, the amount of Co_3O_4 generated gradually added, leading to the decrease of permittivity. This phenomenon will bring about the decrease of dielectric loss and the attenuation loss, which illustrated the decrease of attenuation α is connected with the increase of calcination temperatures. For electromagnetic absorbent, an outstanding absorbing material should consider not only the strong electromagnetic propagation loss, but also the impedance matching. The attenuation constant α and impedance matching Z_r can be described in the following formulas:

$$\alpha=\frac{\sqrt{2}\pi f}{c}\sqrt{(\mu''\varepsilon''-\mu'\varepsilon')+\sqrt{(\mu''\varepsilon''-\mu'\varepsilon')^2+(\mu'\varepsilon''+\mu''\varepsilon')^2}} \quad (6)$$

$$Z_r=Z_{in}/Z_0 \quad (7)$$

where Z_r represents the impedance matching value, Z_0 is the free-space impedance value, Z_{in} is on behalf of the incident impedance matching value, c represents the speed of light. When Z_r = 1, the electromagnetic wave can realize zero reflection on the absorber surface, that is, the absorption effect reaches the best and the condition of $\varepsilon_r=\mu_r$ should be satisfied. According to Figure 7c, the frequency corresponding to the minimum reflection loss of S1 is 11.72 GHz, and the corresponding impedance match at this frequency is 1.06. Similarly, the impedance matching corresponding values of S2 and S3 are 0.53 and 1.00 with the minimum reflection loss, respectively. In addition, the impedance matching values of S3 are closer to 1 at 6-8 GHz Therefore, it illustrated that S3 has achieved almost perfect impedance matching at low frequencies. On the basis of this result, the S3 has better electromagnetic wave absorption performance and attenuation ability at low frequencies. Besides, as shown in Figure 7d, the S1 has more broadband effectively absorption bandwidth of the composites with three different calcination temperatures.

Therefore, the S3 has excellent microwave absorption performance in low frequency, the minimum reflection loss and effective band absorption width of S3 are further analyzed in this paper. In Figure 8a and 8b are minimum RL of S3 with different of matching thicknesses. When the thickness is 4.2 mm, the minimum reflection loss observed at 6.24 GHz is -46.59 dB, indicating elegant electromagnetic wave absorption characteristics. When the thickness of the S3 is reduced to 3.7 mm, the maximum effective absorption bandwidth is 3.04 GHz from 5.84 GHz to 8.88 GHz, at the moment, the minimum reflection loss is -32.13 dB. Compared with the previous work that has been reported in Table 1, the Co_3O_4/CC composites have thinner matching thickness and stronger reflection loss in low frequency.

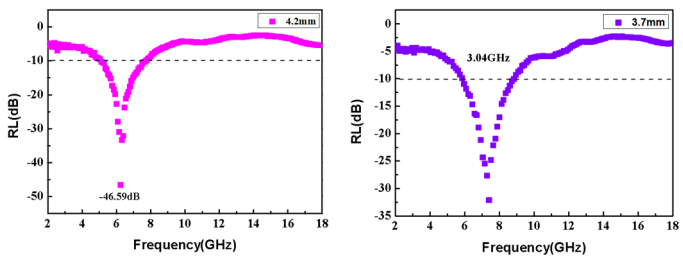

Figure 8. RL curve of S3 at thicknesses of (a) 4.2 mm and (b) 3.7 mm.

Preprints (www.preprints.org) | NOT PEER-REVIEWED | Posted: 1 June 2023 doi:10.20944/preprints202306.0095.v1

Table 1. Microwave absorption performance of the similar materials.

Filler	*RL (dB)*	*Thickness(mm)*	*Effective bandwidth (GHz)*	*Ref.*
$(Zn_{0.8}Mn_{0.2})_2Y$ and Co_2Z department hexagonal ferrite	-15	>5	3.2	40
NiZn Spinel type ferrite	-10	12	0.7	41
Magnesium doped barium ferrite	-10	6.0	3	13
Mg doped lithium zinc ferrite	-39	5.5	6.5	13
Co_3O_4/CC	-46.59	4.2	3.04	**This work**

Based on the above, the Co_3O_4/CC composites have better microwave absorption property with thinner thickness and widely effective absorption bandwidth in low frequency. The possible mechanisms of the microwave absorption are as in Figure 9: firstly, the carbon cloth and Co_3O_4 is a whole, which cause loss for incident electromagnetic wave; secondly, the carbon cloth could provide the network structure that allow more incident wave enter into the internal; finally, when the incident wave pass into the network structure the Co_3O_4 and CC could consume it, and generate dielectric loss. Therefore, the CC and Co_3O_4 synergistically improve the microwave absorption.

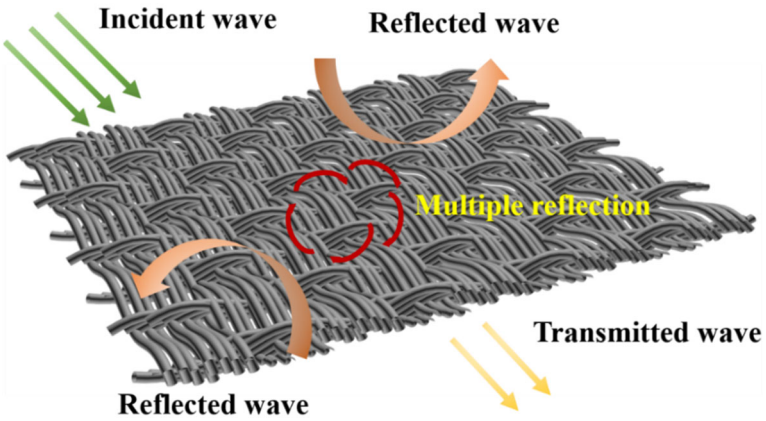

Figure 9. Diagram of microwave attenuation mechanism for Co_3O_4/CC composites.

 doi:10.20944/preprints202306.0095.v1

4. Conclusions

In summary, the precursor Co-MOFs/CC was synthesized by the simple hydrothermal method, and the Co_3O_4/CC derivatives were generated through different calcination temperatures. It was concluded that with the increase of calcination temperature, the electromagnetic wave absorption performance was improved frequency gradually in the low frequency. When the calcination temperature was 500 °C, the minimum reflection loss RL can reach -46.59 dB at 6.24 GHz with 4.2 mm thickness. When the thickness is 3.7 mm, the effective absorption band width was 3.04 GHz in C band, and the minimum reflection loss was -32.13 dB. The synergistical effect of CC and Co_3O_4 made better microwave absorption performance with thinner thickness and widely effective bandwidth in the low frequency. This provides useful inspiration for the growth of absorbing materials on carbon cloth in low frequency, which is worthy of further investigation.

Author Contributions: Conceptualization, B.A. and X.L.; Data curation, B.A.; Formal analysis, B.A. and X.Y.; Investigation, B.A., M.W. and X.L.; Supervision, X.L. and C.F.; Validation, X.L. and C.F.; Visualization, B.A.; Writing-original draft, B.A.; Writing-review and editing, X.L., Z.M. and C.F. All authors approved the final version of the manuscript.

Funding: This work was supported by the National Natural Science Foundation of China (Grant No. 52101218), the Zhejiang Provincial Natural Science Foundation of China (Grant No. LQ22E010004), the Fundamental Research Funds for the Provincial Universities of Zhejiang (Grant No. GK219909299001-009), the National Key R&D Program of China (Grant No. 2022YFB3504804), the National Key R&D Program of China (Grant No. 2021YFA1600203) and the Ten Thousand Talents Plan of Zhejiang Province of China (Grant No. 2019R52014).

Data Availability Statement: The data that support the findings of this study are available from the corresponding authors, upon reasonable request.

Acknowledgments: Thanks to everyone who helped with this work.

Conflicts of Interest: The authors declare no conflict of interest.

References

1. Z, Zhang.; F, Wang, X, Q.; Zhang, W.; Li, J.; G, Guan. Research progress of low frequency wideband thin layer absorbing materials. *J. Funct. Mater.* **2019**,*50(06)* ,606038-606045.
2. F, Wu.; A, Xie.; M, Sun.; Y, Wang.; M, Wang. Reduced Graphene Oxide (RGO) Modified Spongelike Polypyrrole (PPy) Aerogel for Excellent Electromagnetic Absorption. *J. Mater. Chem.* **2015**, *A3(27)*, 14358-14369.
3. Y, Wang.; Z, Peng.; W, Jiang. Controlled synthesis of Fe_3O_4@SnO_2/RGO nanocomposite for microwave absorption enhancement. *Ceram. Int*. **2016**, *42(9)*, 10682-10689.
4. G, Wang.; Y, Wu.; X, Zhang.; Y, Li.; L, Guo.; M, Cao. Controllable Synthesis of Uniform ZnO Nanorods and Their Enhanced Dielectric and Absorption Properties. *J. Mater. Chem.* **2014**, *A2 (23)*, 8644-8651.
5. N, Zhou.; Q, D, An.; Z, Y, Xiao.; S, R, Zhai.; Z, Shi. Solvothermal synthesis of three-dimensional, Fe_2O_3 NPs-embedded CNT/N-doped graphene composites with excellent microwave absorption performance. *RSC. Adv.* **2017**, *7(71)*, 45156-45169.
6. M, S, Cao.; W, L, Song.; Z, L, Hou.; B, Wen.; J, Yuan. The effects of temperature and frequency on the dielectric properties, electromagnetic interference shielding and microwave-absorption of short carbon fiber/silica composites. *Carbon.* **2010**, *48(3)*, 788-796.
7. G, Yilmaz.; K, M, Yam.; C, Zhang.; H, J, Fan.; G, Ho, W. In Situ Transformation of MOFs into Layered Double Hydroxide Embedded Metal Sulfides for Improved Electrocatalytic and Supercapacitive Performance. *Adv. Mater.* **2017**, *29*, 1606814.
8. J, Qian.; T, T, Li.; Y, Hu.; S, Huang. A Bimetallic Carbide Derived from a MOF Precursor for Increasing Electrocatalytic Oxygen Evolution Activity. *Chem. Commun.* **2017**, *53*, 13027-13030.
9. X, Liang.; B, Quan.; Y, Sun.; G, Ji.; Y, Zhang.; J, Ma.; D, Li.; B, Zhang.; Y, Du. Multiple Interfaces Structure Derived from Metal–Organic Frameworks for Excellent Electromagnetic Wave Absorption. *Part. Part. Syst. Charact.* **2017**, *34*, 1700006.

10. Y, Yin.; X, Liu.; X, Wei.; R, Yu.; J, Shui. Porous CNTs/Co Composite Derived from Zeolitic Imidazolate Framework: A Lightweight, Ultrathin, and Highly Efficient Electromagnetic Wave Absorber. *ACS Appl. Mater. Interfaces*. **2016**, *8*, 34686-34698.
11. W, Liu.; Q, Shao.; G, Ji.; X, Liang.; Y, Cheng.; B, Quan.; Y, Du. Metal–Organic Frameworks Derived Porous Carbon-Wrapped Ni Composites with Optimized Impedance Matching as Excellent Lightweight Electromagnetic Wave Absorber. *Chem. Eng. J.* **2017**, *313*, 734-744.
12. J, Ma.; W, Liu.; X, Liang. Nonporous TiO_2/C composites synthesized from directly pyrolysis of a Ti-based MOFs MIL-125(Ti) for efficient microwave absorption. *J. Alloy. Compd*. **2017**, *728*, 138-144.
13. F, Shi.; Y, Hu.; X, Wang. Decomposition of MOFs for the preparation of nano porous Co_3O_4 fibers and sheets with excellent microwave absorption and photocatalytic properties. *Dalton. T*. **2017**, *46(6)*, 1936-1942.
14. W, Liu.; S, J, Tan.; Z, H, Yang.; G, B, Ji. Enhanced Low-Frequency Electromagnetic Properties of MOF-Derived Cobalt through Interface Design. *ACS Appl. Mater. Interfaces.* **2018**, *10. 37*, 31610–31622.
15. Run Yang a.; Jiaqing Yuan a.; Cuihong Yu a.; Kun Yan a.; Yao Fu a.; Hangqing Xie a.; Jian Chen b.; Paul K. Chu c.; Xinglong Wu. Efficient electromagnetic wave absorption by SiC/Ni/NiO/C nanocomposites. *Journal of Alloys and Compounds.* **2020**, *816*, 152519.
16. Peng Miao.; Rui Zhou.; Kaijie Chen*.; Jin Liang.; Qingfu Ban.; and Jie Kong. Tunable Electromagnetic Wave Absorption of Supramolecular Isomer-Derived Nanocomposites with Different Morphology. *Adv. Mater. Interfaces.* **2020**, *7*, 1901820.
17. Q, Zhang.; Y, X, Song.; J, L, Guo.; S, Wu.; N, Chen.; H, G, Fan.; M, Gao.; J, H, Yang.; Z, F, Sheng.; J, H, Lang. One-step hydrothermal synthesis of the modified carbon cloth membrane: Towards visible light driven and self-cleaning for efficient oil-water separation. *Surf. Coat. Tech.* **2021**, *409*.
18. L, M, Yang.; W, D, Chen.; C, H, Sheng.; H, L, Wu.; N, T, Mao.; H, Zhang. Fe/N-codoped carbocatalysts loaded on carbon cloth (CC) for activating peroxymonosulfate (PMS) to degrade methyl orange dyes. *Appl. Surf. Sci.* **2021**, *549*.
19. S, M, Sui.; J, W, Sha.; X.Y. Deng.; S. Zhu.; L.Y. Ma.; C.N. He.; E.Z. Liu.; F. He.; C.S. Shi.; N.Q. Zhao. Boosting the charge transfer efficiency of metal oxides/carbon nanotubes composites through interfaces control, J. Power. Sources. 489(2021).
20. L, Xie.; S, X, Chen.; Y, C, Hu.; Y, Q, Lan.; X, Li.; Q, Deng.; J, Wang.; Z, L, Zeng.; S, G, Deng. Construction of phosphatized cobalt nickel-LDH nanosheet arrays as binder-free electrode for high-performance battery-like supercapacitor device. *J. Alloy. Compd*. **2021**, *858*.
21. Z, T, Nie.; H, J, Zhang.; Y, F, Lu.; C, Y, Han.; Y, H, Du.; Z, C, Sun.; Y, B, Yan.; H, Yu.; X, J, Zhang.; J, X, Zhu. Manipulation of porosity and electrochemical artificial separator interphase for durable lithium-sulfur batteries. *Chem. Eng. J.* **2021**, *409*.
22. Z, F, Liu.; D, D, Ye.; X, Zhu.; S, L, Wang.; R, Chen.; Y, Yang.; Q, Liao. A self-pumping microfluidic fuel cell powered by formatted with Pd coated carbon cloth electrodes. *J. Power. Sources*. **2021**, *490*.
23. K, Q, Dai.; N, Zhang.; L, L, Zhang.; L, X, Yin.; Y, F, Zhao.; B, Zhang. Self-supported Co/CoO anchored on N-doped carbon composite as bifunctional electrocatalyst for efficient overall water splitting. *Chem. Eng. J.* **2021**, *414*.
24. X, H, Luo.; J, Zhang.; C, G, Ci.; R, L, Bai.; D, Y, Shi.; K, M, Xia.; D, W, Wu. Preparation of $NiSe_2$/ CC composite and its electrocatalytic performance for hydrogen evolution. *Micro/Nano Electronic Technology*. **2021**, *58(03)*, 207-213.
25. J, Zhan.; X, Cao.; J, M, Zhou.; G, Xu.; B, Lei.; M, H, Wu. Porous array with CoP nanoparticle modification derived from MOF grown on carbon cloth for effective alkaline hydrogen evolution. *Chem. Eng. J.* **2021**, *416*.
26. Lei Wang.; Xiao Li.; Qingqing Li.; Xuefeng Yu.; Yunhao Zhao.; Jie Zhang.; Min Wang.; and Renchao Che. Oriented Polarization Tuning Broadband Absorption from Flexible Hierarchical ZnO Arrays Vertically Supported on Carbon Cloth. *Small*. **2019**, 1900900.
27. Panbo Liu a*.; Chenyu Zhu b, 1.; Sai Gao a, 1.; Cao Guan b **.; Ying Huang a.; Wenjuan He. N-doped porous carbon nanoplates embedded with CoS_2 vertically anchored on carbon cloths for flexible and ultrahigh microwave absorption. *Carbon.* **2020**, *163*, 348-359.
28. G, P, Wan.; G, Z, Wang.; X, Q, Huang.; H, N, Zhao.; X, Y, Li.; K, Wang.; L, Yu.; X, G. Peng.; Y, Qin. Uniform Fe_3O_4 coating on flower-like ZnO nanostructures by atomic layer deposition for electromagnetic wave absorption. *Dalton Trans.* **2015**, *44(43)*, 18804-18809.
29. Wu L.; Wang Z.; Long Y. Multishelled $Ni_xCo_{3-x}O_4$ hollow microspheres derived from bimetal-organic frameworks as anode materials for high-performance lithium-ion batteries. *Small*. **2017**, *13(17)*, 1604270.
30. Y, W, Zhu.; T, Yu.; C, H, Sow.; Y, J, Liu.; A, T, S, wee.; X, J, Xu.; C, T, Lim.; J, T, L, Thong. Efficient field emission from α-Fe_2O_3 nanoflakes on an atomic force microscope tip. *Appl Phys Lett.* **2005**, *87(2)*, 023103.
31. W, Feng.; Y, Wang.; J, Chen.; L, Wang.; L, Guo.; J, Ou Yang.; D, Jia.; Y, Zhou. Reduced graphene oxide decorated with in-situ growing ZnO nanocrystals: facile synthesis and enhanced microwave absorption properties. *Carbon*. **2016**, *108*, 52–60.

32. J, Yan.; Y, Huang.; Z, Zhang.; X, D, Liu. Novel 3D micro sheets contain cobalt particles and numerous interlaced carbon nanotubes for high-performance electromagnetic wave absorption. *J. Alloys Compd.* **2019**, *785*, 1206−1214.
33. X, H, Liang.; X, M, Zhang.; W, Liu.; D, M, Tang.; B, S, Zhang.; G, B, Ji. A simple hydrothermal process to grow MoS_2 nanosheets with excellent dielectric loss and microwave absorption performance. *J. Mater. Chem. C.* **2016**, *4(28)*, 6816-6821.
34. X, Q, Cui.; X, H, Liang.; W, Liu.; W, H, Gu.; G, B, Ji.; Y, W, Du. Stable microwave absorber derived from 1D customized heterogeneous structures of Fe_3N@C. *Chem. Eng. J.* **2020**, *381*, 122589.
35. X, H, Liang.; B, Quan.; G, B, Ji.; W, Liu.; Y, Cheng.; B, S, Zhang.; Y, W. Du. Novel nanoporous carbon derived from metal-organic frameworks with tunable electromagnetic wave absorption capabilities. *Inorg. Chem. Front.* **2016**, *3 (12)* , 1516−1526.
36. M, Cao.; R, Qin.; C, Qiu.; J, Zhu. Matching Design and Mismatching Analysis towards Radar Absorbing Coatings Based on Conducting Plate. *Mater. Eng.* **2003**, *24 (5)*, 391−396.
37. W, Song.; M, Cao.; Z, Hou.; J, Yuan. High-Temperature Microwave Absorption and Evolutionary Behavior of Multiwalled Carbon Nanotube Nanocomposite. *Scr. Mater*. **2009**, *61 (2)*, 201-204.
38. L, N, Wang.; X, L, Jia.; Y, F, Li.; F, Yang.; L, Q, Zhang.; L, P, Liu.; X, Ren.; H, T, Yang. Synthesis and microwave absorption property of flexible magnetic film based on graphene oxide/carbon nanotubes and Fe3O4 nanoparticles. *J. Mater. Chem.* A. **2014**, *2(36)*, 14940-14946.
39. H, L, Lv.; G, B, Ji.; X, H, Liang.; H, Q, Zhang.; Q, Hai.; Y, W, Du. A novel rod-like MnO_2@Fe loading on graphene giving excellent electromagnetic absorption properties. *J. Mater. Chem. C.* **2015**, *3(19)*, 5056-5064.
40. X, Zhang.; G, Ji.; W, Liu.; B, Quan.; X, H, Liang.; C, M, Shang.; Y, Cheng.; Y, W, Du. Thermal conversion of an Fe_3O_4@metal-organic framework: a new method for an efficient Fe-Co/nanoporous carbon microwave absorbing material. *Nanoscale*. **2015**, *7(30)*, 12932-12942.